JOC The Journal of Organic Chemistry

Article

pubs.acs.org/joc

Mechanism Study of the Intramolecular Anti-Michael Addition of *N*-Alkylfurylacrylacetamides

Haiyan Yuan, Yiying Zheng, and Jingping Zhang*

Faculty of Chemistry, Northeast Normal University, Changchun 130024, China

Supporting Information

ABSTRACT: The mechanism of the intramolecular nucleophilic addition of *N*-alkylfurylacrylacetamides is investigated by density functional theory calculations. Three possible reaction pathways have been considered based on possible conformations of the same reactant, which undergoes three stages, including hydrogen elimination by the base NaH, followed by the nucleophilic addition of N^- on C^α (C^β) via an anti-Michael (Michael) mechanism, and then proton transfer affords the final product **Pr-5** (**Pr-6**). The pathway corresponding to the reactant with the most stable conformation is found to be the most favorable one. The rate-determining step of the intramolecular nucleophilic addition is the nucleophilic addition of N^- on C^α (C^β) featuring a cyclic ring transition state. Solvent effects are considered at the B3LYP/6-31G(d,p) level in solvent DMSO, and the results suggest that the relative reaction trends are consistent with the gas-phase reaction. Furthermore, the difference of the energy barriers explains the origin of the regioselectivity of the experiment. Finally, the effects of the substituent on N1 and C^β to the regioselectivity have been discussed.

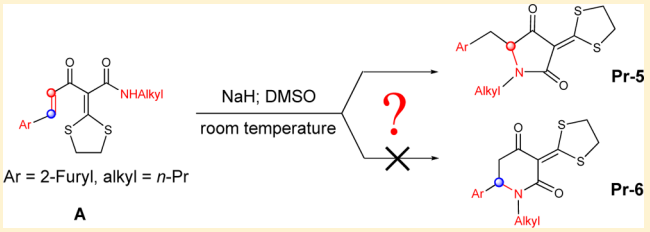

1. INTRODUCTION

The Michael addition of nucleophilic species to α,β-unsaturated systems is a fundamental reaction in organic chemistry, which provides an extremely powerful approach for the synthesis of highly functionalized organic molecules.[1,2] Among the manifold of carbon−heteroatom bond-forming reactions, the Michael addition is of special value for constructing a new bond selectively at the β-position of activated olefins.[3] In recent decades, however, some reactions known as anti-Michael additions,[4−8] contra-Michael additions,[9] reverse additions,[10] nucleophilic α-additions,[11] 1,3-additions,[12] or 1,6-nucleophilic conjugated addition[13] have been reported. In general, the anti-Michael addition reaction includes the following six aspects: (1) transition metal-catalyzed hydrocarbonation of an activated olefin;[14] (2) organocatalytic asymmetric "anti-Michael" reaction of β-ketoesters;[15] (3) addition of alkyllithium to esters, or primary or secondary amides in cinnamic acids through a free radical mechanism;[16] (4) an umpolung of the double bonds of the α,β-unsaturated systems induced by a strong electron-withdrawing group in the β-position;[17] (5) an intramolecular oxo-anti-Michael addition directed by using azide activation at the α-position of *o*-hydroxychalcones;[18] (6) the nonclassical Michael addition of phosphine nucleophiles to the $\alpha(\delta')$-position of an electron-deficient enyne.[13]

Considerable efforts have also been directed at theoretically understanding the factors controlling the regioselectivity of nucleophilic additions at carbon-β vs carbon-α of α,β-unsaturated carbonyl compounds possessing electron-withdrawing substituents at the β-carbon atoms. Shinohara et al.[19] carried out MOPAC calculations for 3,3-bis(trifluoromethyl) acrylate ester along with its nonfluorinated prototype, ethyl crotonate, and 3-trifluoromethyl for both P_z orbital coefficients and LUMO energy levels. Their results showed that the α-position of the investigated compound has an absolute value of the orbital coefficient larger than that of the β-position. In addition, Chatfied et al.[20] have carried out theoretical calculations for the addition of cyanide anion to model several α,β-unsaturated carbonyl compounds to determine the trends of the regioselectivity with respect to properties of the substituents. They found that ΔE^{TS} ($\Delta E^{TS} = E_\alpha{}^{TS} - E_\beta{}^{TS}$, TS = transition state) rather than ΔE^{P} ($E_\alpha{}^{P} - E_\beta{}^{P}$, P = product) are predictive of the regioselectivity.[21] Despite the fact that valuable mechanistic insight has been gleaned from the above-mentioned structural studies, many of the mechanistic details are only related to the intermolecular anti-Michael additions. However, very few research studies have been devoted to the intramolecular anti-Michael additions.[22,23] In 2010, Xu et al.[22] proposed a new concept, namely, polarity-reversible conjugate addition. In particular, they found that the intramolecular conjugate addition reactions of *N*-alkylfurylacrylacetamide (**A**) (1.0 mol) with an alkyl on the amide nitrogen were obtained in 89% yields with NaH (1.0 equiv) in DMSO (5.0 mL) at room temperature for 0.5 h (Scheme 1). This approach brings new insight to conjugate addition chemistry, but a detailed theoretical investigation concerning the mechanism of the intramolecular anti-Michael addition of *N*-alkylfurylacrylacetamide has not been performed so far. Therefore, we take **A** as starting material to investigate the origin of regioselectivity for

Received: August 31, 2012
Published: September 11, 2012

 © 2012 American Chemical Society dx.doi.org/10.1021/jo3018796 | J. Org. Chem. 2012, 77, 8744−8749

Scheme 1. Intramolecular Aza-anti-Michael Addition of A

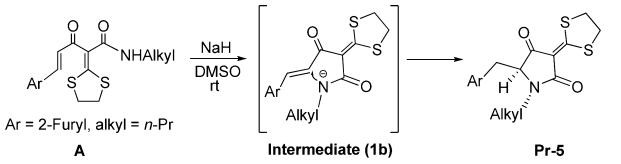

intramolecular aza-anti-Michael cycloaddition without any additional catalyst.

2. COMPUTATIONAL DETAILS

All calculations were performed using the Gaussian 09 program package.[24] Geometry optimizations were carried out using the well-established B3LYP exchange-correlation functional,[3] together with the standard 6-31G(d,p) basis set. The same theoretical level was also used for the frequency calculations. Therefore, the zero-point vibrational energy (ZPE) contributions at the 6-31G(d,p) level were accounted for all the energy values in the current work. The intrinsic reaction coordinate (IRC)[25] paths were traced to check the energy profiles connecting each TS to the two associated minima of the proposed mechanism using the second-order González–Schlegel integration method.[25a,26] The electronic structures of stationary points and bond orders (Wiberg indexes) were analyzed by the NBO method.[27] To investigate the effect of basis sets, we calculated the single-point energy at the B3LYP/6-311+G(d,p) level of theory to confirm the qualitative results at the B3LYP/6-31G(d,p) level.

The solvent effects were considered by B3LYP/6-31G(d,p) single-point calculations with gas-phase-optimized geometry using a self-consistent reaction field (SCRF)[28] based on the polarizable continuum model (PCM) of the Tomasi group.[29] As the solvent used in the experimental work is DMSO, we selected its dielectric constant at 298.0 K, ε = 46.826.

To model the hydrogen shift reaction in the bulk water, the calculations were performed with the ONIOM (B3LYP/6-31G-(d,p):PM6) approach as implemented in the Gaussian 09 program.[30] The system consisted of **Int6** (**Int6′**) plus 193 water molecules contained in a periodically replicated cube box of dimensions of 18.0 × 18.0 × 18.0 Å.

3. RESULTS AND DISCUSSION

For the α,β-unsaturated system **A**, the four possible conformations possessing lower energies are considered and the optimized structures of **A**, **A-1**, **A-2**, and **A-3** are shown in Figure 1. The dihedral angle C3–C2–N1–C1 of these four conformations are −179.3°, −6.7°, −22.7°, and −178.1°, respectively. The calculated energy of **A** is 6.0, 3.0, and 2.3 kcal/mol lower than that of **A-1**, **A-2**, and **A-3**, respectively. Thus **A** is the most stable conformation for this reaction.

In this paper, we have investigated three possible reaction pathways of intramolecular nucleophilic addition of **A** with

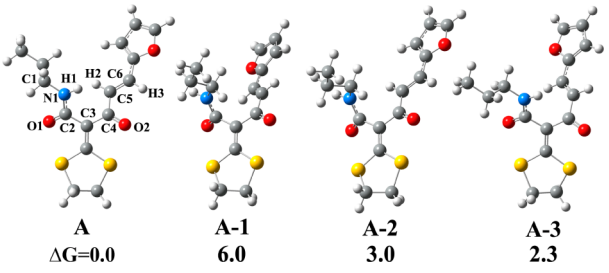

Figure 1. Optimized structures and relative energies (kcal/mol) of the four conformations **A**, **A-1**, **A-2**, **A-3**. S: yellow, N: light blue, C: gray, O: red, H: white.

three different conformations: channel-1, channel-2, and channel-3 by using **A**, **A-1**, and **A-2** as reactants, respectively. The channel related to reactant **A-3** was not fully located because the intermediate was very stable (see Figure S1 in Supporting Information for detail). Each channel contains two pathways, pathway n-f and pathway n-s, where n = 1, 2, or 3 for channel number, and f or s denotes five-membered or six-membered ring, corresponding to anti- or Michael addition. The intramolecular anti/or Michael addition of **A** could be described as a three-stage process involving H1-elimination promoted by NaH base (stage 1), nucleophilic addition of N^- to C^α (C^β), i.e., C5 (C6) via anti-Michael (Michael) mechanism (stage 2), and the proton transfer and the product (**Pr-5**/**Pr-6**) formation (stage 3).

3.1. Three Stages of Channel-1. *Stage 1. H1-Elimination Promoted by NaH Base.* The energy profile and the corresponding geometry structures for channel-1 are given in Figures 2–6. The relative free energies (ΔG) are listed with respect to the starting materials (**A** + NaH) for all the species. The initial step of stage 1 for channel-1 is the electrostatic attraction between the negative H4 of NaH and positive H1 of **A** and the formation of complex **Com1**.[31] **Com1** is more stable in free energy than **A** + NaH by 13.0 kcal/mol. Hence, the electrostatic attraction between H4 and H1 can facilitate the hydrogen elimination. The intermediate **Int1** is formed by the nucleophilic attack of NaH to the H1 of **A** via a low free energy barrier ($\Delta\Delta G^{\ddagger}$) transition state **TS1** of 6.5 kcal/mol. The H1-elimination process is illustrated by the gradually shortened H1–H4 distance, from 1.76 Å in **Com1** to 0.75 Å in **Int1**, and weakened bonds N1–H1 (1.04 Å vs 3.59 Å) and H4–Na1 (1.97 Å vs 2.66 Å) from **Com1** to **Int1** (see Figure 3). The ΔG value of **Int1** is −26.2 kcal/mol lower than that of **A** + NaH. In the second step of stage 1, the H_2 molecule for **Int1** is released, forming **Int2**. This is followed by two conformational changes from **Int2**, giving two intermediates (**Int3** and **Int4**). The $\Delta\Delta G^{\ddagger}$ values for these two conformational changes are 9.0 kcal/mol, respectively (see Figure 2).

Stage 2. The Nucleophilic Addition of N^- to C^α (C^β). The intermediate **Int4** facilitates the attack of the nucleophilic N1 to C^α (i.e., C5), which undergoes an anti-Michael addition mechanism (see Figure 2, pathway 1-f). Then the five-membered ring closure affords the intramolecular cycloadduct **Int5** via a cyclic transition state **TS4-f**, with the $\Delta\Delta G^{\ddagger}$ value of 20.2 kcal/mol. Herein, the N1–C5 bond distance shortens from 3.59 Å of **Int4** to 1.78 Å of **TS4-f** and then to 1.47 Å of **Int5**, and the C5–C6 bond distance elongates from 1.35 Å at **Int4** to 1.41 Å at **TS4-f** and then to 1.48 Å at **Int5**. These changes imply that the N1–C5 bond is gradually formed and that the C5–C6 bond is gradually broken in the intramolecular nucleophilic addition processes. This is followed by a conformational change from **Int5** to a more stable intermediate **Int6** for further reaction (see Figure 4).

Meanwhile, we also explored the corresponding Michael addition reaction (pathway 1-s) for comparison. The adduct **Int5′** is formed via a six-membered ring transition state **TS4′-s**. In Figure 2, the formation of the six-membered ring transition state **TS4′-s** requires 22.4 kcal/mol of the $\Delta\Delta G^{\ddagger}$ value, which is 2.2 kcal/mol higher than that of **TS4-f** (20.2 kcal/mol). Furthermore, the N1–C5 bond distance in **TS4-f** is shorter than that of the N1–C6 bond in **TS4′-s** (see Figure 4). The N1–C6 and C5–C6 bond lengths/distances change from 3.54 Å and 1.35 Å in **Int4** to 1.49 Å and 1.50 Å in **Int5′**, respectively. Both the energy barriers and C–N bond length changes

dx.doi.org/10.1021/jo3018796 | J. Org. Chem. 2012, 77, 8744–8749

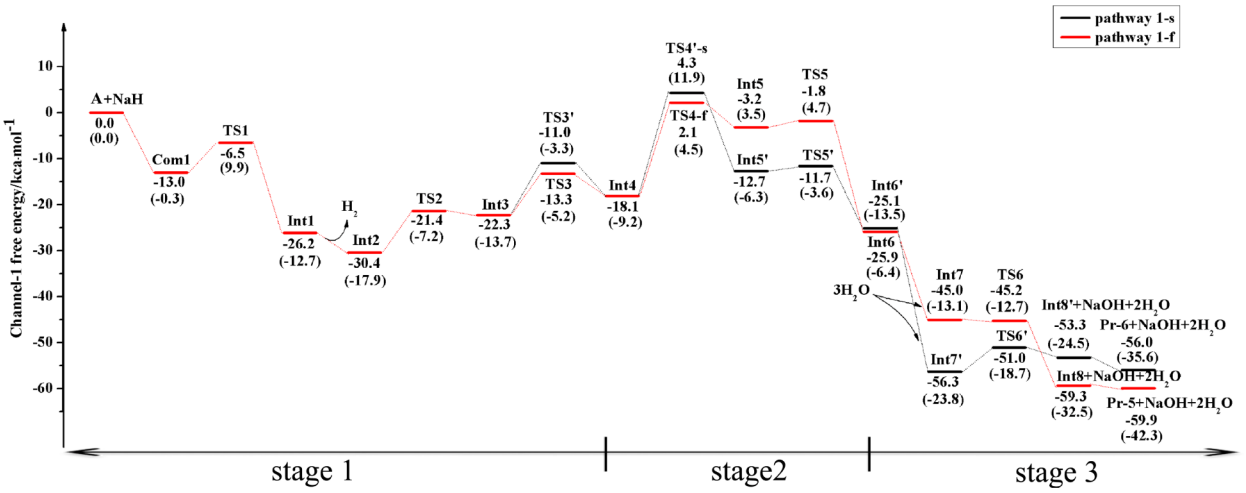

Figure 2. Free energy profiles of pathways 1-f (for anti-Michael mechanism, in red) and 1-s (for Michael mechanism, in black) for reaction channel-1. Values in kcal/mol are free energies in gas and solution (in parentheses), respectively.

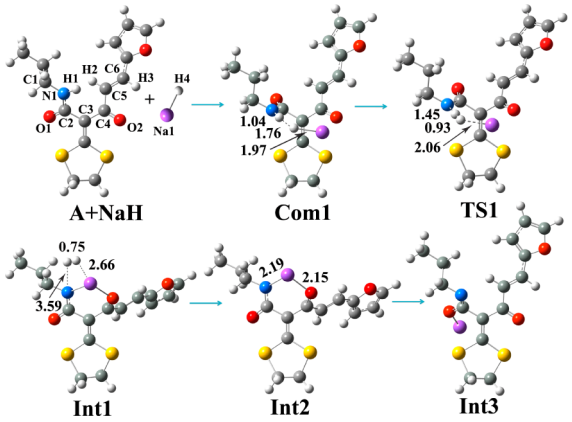

Figure 3. Selected optimized structures for stage 1 of channel-1; bond lengths and distances are in angstroms. (S: yellow, N: light blue, C: gray, O: red, H: white, Na: purple).

indicate that the nucleophilic attack at C^{α} (C5) position is more favorable than at C^{β} (C6).

The extent of the bond-formation along a reaction pathway is provided by the concept of bond order (BO). The BO values of the C−N forming-bonds at the **TSs** are 0.56 (N1−C5) at **TS4-f** and 0.43 (N1−C6) at **TS4′-s**. These values suggest that the bond formation at the α-conjugated position (C5) of **A** is more favored than that at the β-conjugated position (C6).

*Stage 3. Proton Transfer and Product (**Pr-5/6**) Formation.* Because the resulting mixture was poured into ice−water (50 mL) under stirring in the experiment, we hypothesized that hydrogen can transfer from the water molecule to the C^{β}/C^{α} anion of **Int6**/**Int6′**. Therefore, we carried out the ONIOM (B3LYP/6-31G(d,p):PM6) calculation to mimic the reaction in the bulk water.[30] It was also recommended that the minimal of three-water cluster can be efficiently used to simulate the effect of water.[32] Hence, a three-water cluster in the reaction center was chosen. As shown in Figure 5a, the hydrogen bond between C6 and H1′ is 1.90 Å, and the bond distance of Na1−O1′ is 2.41 Å while the C5−H1′ and Na1−O1′ distances are 2.30 Å and 2.53 Å, respectively (see Figure 5b). The optimized water complex (**Int7**/**Int7′**) is more stable than **Int6**/**6′**+**3H$_2$O**, with a ΔG value (19.1/31.2 kcal/mol) lower than that of **Int6**/**6′**+**3H$_2$O**.

In the following step, H1′ in the three-water cluster of **Int7** shifts from O1′ to C6 and generates **Int8** via transition state **TS6**. The corresponding $\Delta\Delta G^{\ddagger}$ value is −0.2 kcal/mol, which

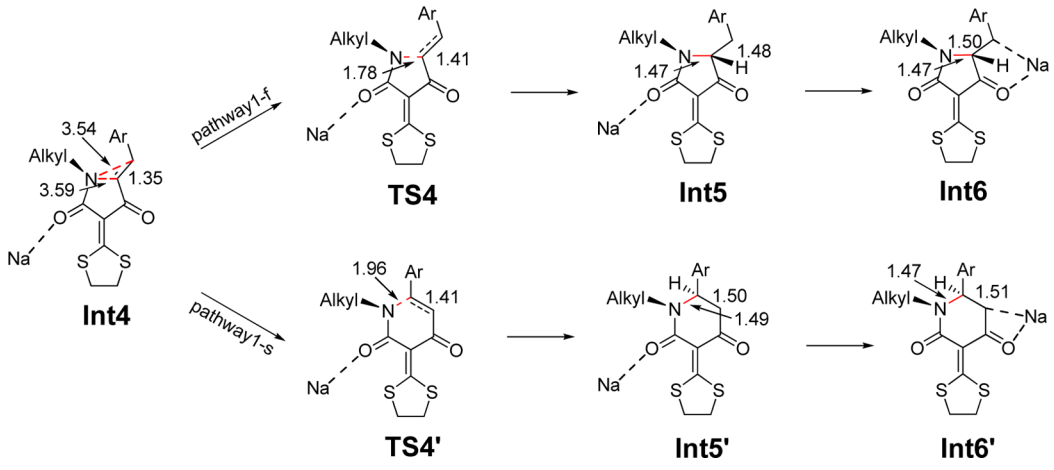

Figure 4. Optimized structures of key stationary points for step 2 along with the key bond distance in angstroms. Other optimized structures are given in the Supporting Information.

dx.doi.org/10.1021/jo3018796 | J. Org. Chem. 2012, 77, 8744−8749

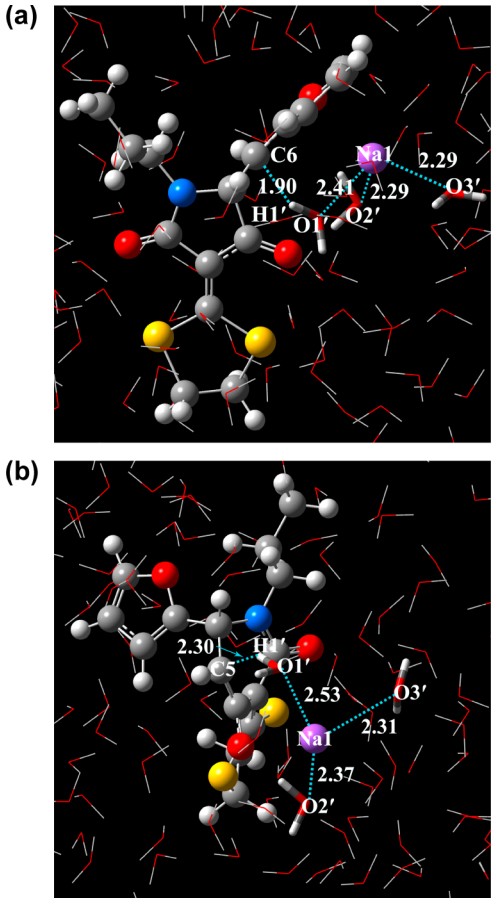

Figure 5. (a) The hydrogen bond distances between the C^{β} (C6) in **Int6** and three solvent water molecules were chosen at the B3LYP/6-31G(d,p) level. (b) The hydrogen bond distance between the C^{α} (C5) in **Int6′** and three solvent water molecules were chosen at the B3LYP/6-31G(d,p) level.

is a barrier-free proton transfer (BFPT) process. This can be ascribed to the assisted water cluster acting as a proton transfer bridge.[33] The $\Delta\Delta G^{\ddagger}$ value of proton transfer for the Michael addition process is 5.3 kcal/mol, which is higher than that of the anti-Michael addition. Figure 6 shows that the newly formed C6−H1′ bond causes the elongation of the O1′−H1′ bond from 1.01 Å to 2.02 Å and the decrease of the C6−H1′ bond from 1.90 Å to 1.10 Å. The bond distance variations indicate that the O1′−H1′ bond is broken and the C6−H1′ bond is formed during rearrangement process. Furthermore, the bond distance of Na1−O1′ is 2.41 Å in **Int7**, which shortens to 2.29 Å in **TS6** and to 2.16 Å in **Int8**. This suggests that the Na^{+} plays an important role in assisting the hydrogen shift in stage 3 (see Figure 6). Meanwhile, a similar trend can be found in the corresponding Michael addition process (Figure 6). Finally, the product **Pr-5/6** is formed through the tautomerization of **Int8/8′**. The ΔG value for **Pr-5** is 3.9 kcal/mol lower than that for **Pr-6**. Hence, the anti-Michael addition is more favorable than the Michael addition thermodynamically.

For a deeper understanding of the proton transfer process, we evaluated the natural population analysis (NPA) for both **TS6** and **TS6′**, as presented in Figure 7. We found a charge

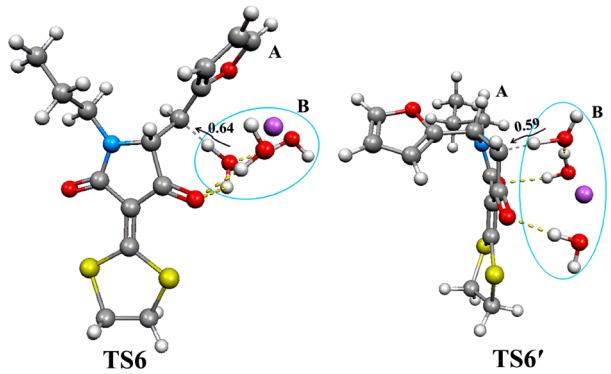

Figure 7. The NPA charges for **TS6** and **TS6′** at the B3LYP/6-31G(d,p) level.

transfer (CT) from the assisted water cluster (part B) to the species (part A) for both **TS6** and **TS6′**. The CT from B to the A part in **TS6** is 0.64e, which is 0.05e greater than that in **TS6′** (0.59e). This indicates that **TS6** is stabilized by the three-water cluster in comparison with **TS6′**.

Figure 2 illustrates the whole intramolecular nucleophilic addition mechanism of channel-1, including the three stages: (1) H1 elimiantion by base NaH (from **Com1** to **Int4**), (2) the nucleophilic addition of $N1^{-}$ on C^{α}/C^{β} (from **Int4** to **Int6**), (3) the hydrogen shift (from **Int6** to **Pr-5/Pr-6**). The step for the ring closure is the rate-determining step. Moreover, the

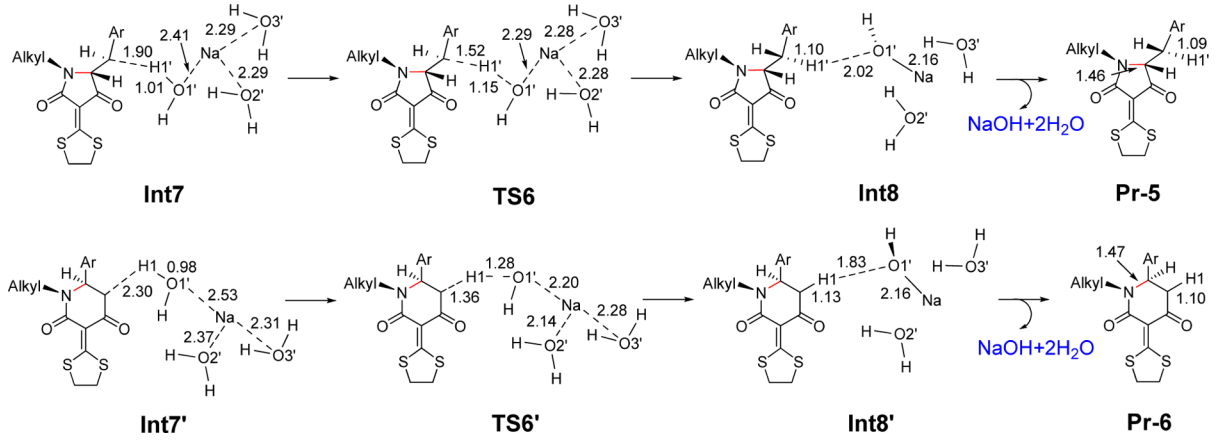

Figure 6. B3LYP/6-31G(d,p) structure parameters for the stationary structures found in step 3 for channel-1. Distances are given in angstroms.

dx.doi.org/10.1021/jo3018796 | J. Org. Chem. 2012, 77, 8744−8749

pathway 1-f is more feasible than pathway 1-s both kinetically and thermodynamically.

Furthermore, we also calculated channel-2 and channel-3, which also undergo three stages, similar to that for channel-1 (Figures S3 and S4 in Supporting Information). The rate-determination step for both channels is the nucleophilic attack of N^- on C^α (C^β) as channel-1. The calculated results for both channel-2 and channel-3 also reveal that each anti-Michael addition is more favorable than the Michael addition process. The $\Delta\Delta G^{\ddagger}$ values for pathways 2-f of channel-2 and 3-f of channel-3 are 25.0 and 28.1 kcal/mol, respectively. They are 4.8 and 7.9 kcal/mol higher than that for pathway 1-f of channel-1, respectively. The higher $\Delta\Delta G^{\ddagger}$ values for step 2 of channel-2 and channel-3 indicate that channel-1 is the most favorable one. Consequently, we will only discuss channel-1.

3.2. Effects of the Substituents R^1 and R^2 on the Regioselectivity. To investigate the origin of the regioselectivity, the substituent effects of the R^1 and R^2 groups are explored. The results in Table 1 show that the substituents on N1 or C^β can affect the reaction barriers. The regioselectivity can be changed by a stronger electron-withdrawing (EW) group R^1 (when R^2 = *n*-Pr), i.e., the anti-Michael reaction is the favorable one. As seen from Table 1, the $\Delta\Delta E^{TS}$ values of compounds **1** (−6.4 kcal/mol), **2** (−3.2 kcal/mol), and **5** (−3.4 kcal/mol) are negative. However, the $\Delta\Delta E^{TS}$ value for both compound **3** (1.4 kcal/mol) and **4** (10.9 kcal/mol) are positive. Hence, the relatively weak EW group (CN) and the electron-donating (ED) group (CH_3) at C^β could not reverse the polarity of the carbon−carbon double bond in compounds **3** and **4**.[20] Therefore, compound **1** (R^1 = NO_2) is the best candidate for the anti-Michael addition if R^2 = *n*-Pr.

Table 1. Calculated Substituent Effects for R^1 and R^2 [a]

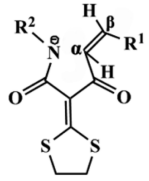

compound	R^1	R^2	$\Delta\Delta E^{TS}$
1	NO_2	*n*-Pr	−6.4
2	CHO	*n*-Pr	−3.2
3	CN	*n*-Pr	1.4
4	CH_3	*n*-Pr	10.9
5	2-thienyl	*n*-Pr	−3.4
6	2-furyl	OMe	−8.7
7	2-furyl	*t*-Bu	11.0
8	2-furyl	Ph	9.1
9	NO_2	OMe	−11.3

[a] $\Delta\Delta E^{TS} = \Delta E_\alpha^{TS} - \Delta E_\beta^{TS}$ (positive for β-addition, negative for α-addition), and values are in kcal/mol.

The substituent R^2 (when R^1 = 2-furyl) on the N1 has a stronger effect on $\Delta\Delta E^{TS}$ than R^1. Because OMe, *t*-Bu, and Ph groups are ED groups, the $\Delta\Delta E^{TS}$ value for the corresponding compounds **6**−**8** are expected to be negative, however, the calculated results indicate that the $\Delta\Delta E^{TS}$ values of compounds **7** (R^2 = *t*-Bu) and **8** (R^2 = Ph) are 11.0 and 9.1 kcal/mol, respectively. This can be explained by the steric hindrance effect between *t*-Bu/Ph and H^α of compounds **7** and **8**. As a consequence, compound **6** (R^2 = OMe) is a better candidate for the anti-Michael reaction. Note that the calculated results in Table 1 suggest that compound **9** (R^1 = NO_2 and R^2 = OMe) is a better substrate for the experiment. This is due to the strong ED group OMe on R^2 that increases the nucleophilicity of N1, and the strong EW group NO_2 on C^β, which are enough to reverse the regioselectivity of nucleophilic addition from the classical β-addition to an α-addition.

3.3. Solvent Effect. Because this reaction was carried out in DMSO, we considered the solvent effect by single-point calculations on the gas-phase geometries using the PCM model. As shown in Figure 2, the $\Delta\Delta G^{\ddagger}$ value for the nucleophilic attack process is 13.7 kcal/mol for pathway 1-f in DMSO solution, which is 6.5 kcal/mol lower than that in the gas phase. Hence, this reaction is more favorable in DMSO than in the gas phase. This is in excellent agreement with the experimental observations where the reaction was accomplished at room temperature in 30 min. The $\Delta\Delta G^{\ddagger}$ value for the nucleophilic attack process is 21.1 kcal/mol for pathway 1-s, which is 7.4 kcal/mol higher than that for pathway 1-f. It was suggested that a free energy barrier difference of 5.0 kcal/mol can almost exclude the unfavorable reaction channel for the kinetically controlled reaction with two reaction channels.[34] Hence, our results imply that the anti-Michael addition is more favorable than the Michael addition pathway, considering the solvent effect.

4. CONCLUSION

In summary, we have studied the detailed reaction mechanism of the intramolecular nucleophilic addition of *N*-alkylfurylacrylacetamide and found three possible reaction channels at the B3LYP/6-31G(d,p) level according to the different conformations of reactant. Channel-1 is the most energy-favorable one among the three possible reaction channels. The whole reaction take place through three stages, including H-elimination promoted by NaH base, the nucleophilic addition of N^- to C^α (C^β) via anti-Michael (Michael) mechanism, and the proton transfer and product (**Pr-5**/**6**) formation. The step for the nucleophilic addition of N^- to C^α (C^β) is the rate-determining step. In the solvent of DMSO, the $\Delta\Delta G^{\ddagger}$ value for the nucleophilic attack at C^α (C5) position is 7.4 kcal/mol lower than that at C^β (C6). This is in excellent agreement with the experimental findings.

The analysis of the $\Delta\Delta E^{TS}$ provides a further explanation about the different regioselectivity. In addition, we also investigated the influence of the EW and ED groups on N1 and C^β on the regioselectivity. The results indicated that compound **9** is predicted to be the best substrate compared with the others for anti-Michael addition. This is due to a cooperative effect of the strong ED and EW character on N1 and C^α,C^β, favoring α-addition over β-addition in α,β-unsaturated systems.

■ ASSOCIATED CONTENT

Supporting Information

The Gibbs free energies of all reported channel-1 structures for basis set 6-311+G(d,p). Free energy profiles for channel-2, channel-3, and channel-4 and energies of reactants, various intermediates, transition states, and corresponding Cartesian coordinates. This material is available free of charge via the Internet at http://pubs.acs.org.

■ AUTHOR INFORMATION

Corresponding Author

*E-mail: zhangjp162@nenu.edu.cn.

Notes

The authors declare no competing financial interest.

■ ACKNOWLEDGMENTS

Financial support from the National Natural Science Foundation of China (21173037) and the Graduated Students Innovation Foundation (09ssxt124) is gratefully acknowledged.

■ REFERENCES

(1) (a) Perlmutter, P. *Conjugate Addition Reactions in Organic Synthesis*; Pergamon: Oxford, 1992. (b) Jung, M. E. *Comprehensive Organic Synthesis*; Trost, B. M., Fleming, I., Semmelhack, M. F., Eds.; Pergamon: Oxford, 1991; Vol. *4*, pp 1−67.

(2) (a) Enders, D.; Saint-Dizier, A.; Lannou, M.-I.; Lenzen, A. *Eur. J. Org. Chem.* **2006**, 29−49 (phospha-Michael addition). (b) Nising, C. F.; Brase, S. *Chem. Soc. Rev.* **2008**, *37*, 1218−1228 (oxa-Michael addition). (c) Sun, X.-L.; Tang, Y. *Acc. Chem. Res.* **2008**, *41*, 937−948 (ylide-initiated Michael addition−cyclization reactions). (d) Enders, D.; Luttgen, K.; Narine, A. A. *Synthesis* **2007**, 959−980 (asymmetric sulfa-Michael addition).

(3) Lewandowska, E.; Chatfield, D. C. *Eur. J. Org. Chem.* **2005**, 3297−3303.

(4) (a) Coyanis, E. M.; Della Védova, C. O.; Haas, A.; Winter, M. *J. Fluorine Chem.* **2002**, *117*, 185−192. (b) Keese, R.; Hinderling, C. *Synthesis* **1996**, 695−696. (c) Hass, A.; Lieb, M.; Schelvis, M. *J. Fluorine Chem.* **1997**, *83*, 133−143. (d) Martin, V.; Molines, H.; Wakselman, C. *J. Org. Chem.* **1992**, *57*, 5530−5532. (e) Eberle, M. K.; Keese, R. *Helv. Chim. Acta* **1998**, *81*, 182−186.

(5) Bumgardner, C. L.; Bunch, J. E.; Whangbo, M. H. *J. Org. Chem.* **1986**, *51*, 4082−4083.

(6) (a) Back, T. G.; Bethell, R. J.; Parvez, M.; Wehrli, D. *J. Org. Chem.* **1998**, *63*, 7908−7919. (b) Back, T. G.; Wehrli, D. *Tetrahedron Lett.* **1995**, *36*, 4737−4740.

(7) Klumpp, G. W.; Mierop, A. J. C.; Vrielink, J. J.; Brugman, A.; Schakel, M. *J. Am. Chem. Soc.* **1985**, *107*, 6740−6742.

(8) (a) Rudorf, W.-D.; Schwarz, R. *Synlett* **1993**, 369−374. (b) Rudorf, W.-D.; Schwarz, R. *Tetrahedron Lett.* **1987**, *28*, 4267−4270.

(9) (a) Bremand, N.; Marek, I.; Normant, J. F. *Tetrahedron Lett.* **1999**, *40*, 3379−3382. (b) Bremand, N.; Marek, I.; Normant, J. F. *Tetrahedron Lett.* **1999**, *40*, 3383−3386.

(10) (a) Kamimura, A.; Murakami, N.; Yokota, K.; Shirai, M.; Okamoto, H. *Tetrahedron Lett.* **2002**, *43*, 7521−7523. (b) Kamimura, A.; Murakami, N.; Kawahara, F.; Yokota, K.; Omata, Y.; Matsuura, K.; Oishi, Y.; Morita, R.; Mitsudera, H.; Suzukawa, H.; Kakehi, A.; Shirai, M.; Okamoto, H. *Tetrahedron* **2003**, *59*, 9537−9546.

(11) (a) Trost, B. M.; Dake, G. R. *J. Am. Chem. Soc.* **1997**, *119*, 7595−7596. (b) Shvo, Y.; Arisha, A. H. I. *J. Org. Chem.* **2001**, *66*, 4921−4922.

(12) (a) Plunian, B.; Vaultier, M.; Mortier, J. *Chem. Commun.* **1998**, 81−82. (b) Aurell, M. J.; Banuls, M. J.; Mestres, R.; Munoz, E. *Tetrahedron* **1999**, *55*, 831−846. (c) Aurell, M. J.; Banuls, M. J.; Mestres, R.; Munoz, E. *Tetrahedron* **1999**, *57*, 1067−1074.

(13) Deng, J.-C.; Chuang, S.-C. *Org. Lett.* **2011**, *13*, 2248−2251.

(14) Shim, J.-G.; Park, J. C.; Cho, C. S.; Shim, S. C.; Yamamoto, Y. *Chem. Commun.* **2002**, 852−853.

(15) (a) Alemán, J.; Reyes, E.; Richter, B.; Overgaard, J.; Jorgensen, K. A. *Chem. Commun.* **2007**, 3921−3923. (b) Yang, H.; Wong, M. W. *J. Org. Chem.* **2011**, *76*, 7399−7405.

(16) (a) Klumpp, G. W.; Mierop, A. J. C.; Vrielink, J. J.; Brugman, A.; Schakel, M. *J. Am. Chem. Soc.* **1985**, *107*, 6740−6742. (b) Crossland, I. *Acta Chem. Scand. B* **1975**, *29*, 468−470. (c) Aurell, M. a. J.; Banuls, M. a. J.; Mestres, R.; Munoz, E. *Tetrahedron* **2001**, *57*, 1067−1074.

(17) (a) Ponticello, G. S.; Freedman, M. B.; Habecker, C. N.; Holloway, M. K.; Amato, J. S.; Conn, R. S.; Baldwin, J. J. *J. Org. Chem.* **1988**, *53*, 9−13. (b) Coyanis, E. M.; Della Védova, C. O.; Haas, A.; Winter, M. *J. Fluorine Chem.* **2002**, *117*, 185−192. (c) Reinhart, K.; Christian, H. *Synthesis* **1996**, 695−696.

(18) Bi, X.; Zhang, J.; Liu, Q.; Tan, J.; Li, B. *Adv. Synth. Catal.* **2007**, *349*, 2301−2306.

(19) Shinohara, N.; Haga, J.; Yamazaki, T.; Kitazume, T.; Nakamura, S. *J. Org. Chem.* **1995**, *60*, 4363−4374.

(20) Chatfield, D. C.; Augsten, A.; D'Cunha, C.; Lewandowska, E.; Wnuk, S. F. *Eur. J. Org. Chem.* **2004**, 313−322.

(21) Lewandowska, E. *Tetrahedron* **2007**, *63*, 2107−2122.

(22) Li, Y.; Xu, X.; Tan, J.; Liao, P.; Zhang, J.; Liu, Q. *Org. Lett.* **2010**, *12*, 244−247.

(23) (a) Bi, X.; Zhang, J.; Liu, Q.; Tan, J.; Li, B. *Adv. Synth. Catal.* **2007**, *349*, 2301−2306. (b) Li, Y.; Liang, F.; Bi, X.; Liu, Q. *J. Org. Chem.* **2006**, *71*, 8006−8010.

(24) Frisch, M. J.; Trucks, G. W.; Schlegel, H. B.; Scuseria, G. E.; Robb, M. A.; Cheeseman, J. R.; Scalmani, G.; Barone, V.; Mennucci, B.; Petersson, G. A.; Nakatsuji, H.; Caricato, M.; Li, X.; Hratchian, H. P.; Izmaylov, A. F.; Bloino, J.; Zheng, G.; Sonnenberg, J. L.; Hada, M.; Ehara, M.; Toyota, K.; Fukuda, R.; Hasegawa, J.; Ishida, M.; Nakajima, T.; Honda, Y.; Kitao, O.; Nakai, H.; Vreven, T.; Montgomery, J. A., Jr.; Peralta, J. E.; Ogliaro, F.; Bearpark, M.; Heyd, J. J.; Brothers, E.; Kudin, K. N.; Staroverov, V. N.; Kobayashi, R.; Normand, J.; Raghavachari, K.; Rendell, A.; Burant, J. C.; Iyengar, S. S.; Tomasi, J.; Cossi, M.; Rega, N.; Millam, N. J.; Klene, M.; Knox, J. E.; Cross, J. B.; Bakken, V.; Adamo, C.; Jaramillo, J.; Gomperts, R.; Stratmann, R. E.; Yazyev, O.; Austin, A. J.; Cammi, R.; Pomelli, C.; Ochterski, J. W.; Martin, R. L.; Morokuma, K.; Zakrzewski, V. G.; Voth, G. A.; Salvador, P.; Dannenberg, J. J.; Dapprich, S.; Daniels, A. D.; Farkas, Ö.; Foresman, J. B.; Ortiz, J. V.; Cioslowski, J.; Fox, D. J. *Gaussian 09*; Gaussian, Inc., Wallingford CT, 2009.

(25) (a) Gonzalez, C.; Schlegel, H. B. *J. Phys. Chem.* **1990**, *94*, 5523−5527. (b) Gonzalez, C.; Schlegel, H. B. *J. Chem. Phys.* **1989**, *90* (4), 2154−2161.

(26) Gonzalez, C.; Schlegel, H. B. *J. Chem. Phys.* **1991**, *95*, 5853−5860.

(27) (a) Reed, A. E.; Curtiss, L. A.; Weinhold, F. *Chem. Rev.* **1988**, *88*, 899−926. (b) Reed, A. E.; Weinstock, R. B.; Weinhold, F. *J. Chem. Phys.* **1985**, *83*, 735−746.

(28) (a) Tomasi, J.; Persico, M. *Chem. Rev.* **1994**, *94*, 2027−2094. (b) Simkin, B. Y.; Sheikhet, I. *Quantum Chemical and Statistical Theory of Solutions-A Computational Approach*; Ellis Horwood: London, 1995.

(29) (a) Cancès, E.; Mennucci, B.; Tomasi, J. *J. Chem. Phys.* **1997**, *107*, 3032−3041. (b) Cossi, M.; Barone, V.; Cammi, R.; Tomasi, J. *Chem. Phys. Lett.* **1996**, *255*, 327−335. (c) Barone, V.; Cossi, M.; Tomasi, J. *J. Comput. Chem.* **1998**, *19*, 404−417.

(30) Zheng, Y.; Zhang, J. *J. Phys. Chem. A* **2010**, *114*, 4325−4333.

(31) Kudoh, T.; Mori, T.; Shirahama, M.; Yamada, M.; Ishikawa, T.; Saito, S.; Kobayashi, H. *J. Am. Chem. Soc.* **2007**, *129*, 4939−4947.

(32) (a) Kovács, G.; Schubert, G.; Joó, F.; Pápai, I. *Organometallics* **2005**, *24*, 3059−3065. (b) Chu, H. S.; Xu, Z.; Ng, S. M.; Lau, C. P.; Lin, Z. *Eur. J. Inorg. Chem.* **2000**, 993−1000.

(33) Zheng, Y.; Zhang, J. *ChemPhysChem.* **2010**, *11*, 65−69.

(34) Zhao, L.; Chen, X. Y.; Ye, S.; Wang, Z.-X. *J. Org. Chem.* **2011**, *76*, 2733−2743.